CONF-881151--48

DE89 004278

THE ARGONNE FRAGMENT MASS ANALYZER

Cary N. DAVIDS and James D. LARSON

Physics Division, Argonne National Laboratory, Argonne, IL 60439 U.S.A.*

Abstract

The Fragment Mass Analyzer (FMA) is currently under construction at the ATLAS facility. The FMA is a eight-meter long recoil mass spectrometer which will be used to separate nuclear reaction products from the primary heavy-ion beam and disperse them by A/q (mass/charge) at the focal plane. The FMA will be used in many different types of experiments. Gamma rays originating from very weak fusion-evaporation channels can be observed in coincidence with the recoil nucleus identified at the FMA focal plane. Production and decay of nuclei far from stability will be studied at the focal plane by implanting exotic recoils directly into detectors or by using a fast tape transport system. The FMA will also be used for reaction mechanism studies. A radioactive beam facility behind the focal plane is planned, which will allow beta-NMR and nuclear moment measurements to be made. The FMA will utilize the wide range of beams and intensities to be provided by the new ECR-positive ion injector also under construction at ATLAS.

---

*Work supported by the U. S. Department of Energy, Nuclear Physics Division, under Contract W-31-109-Eng-38.

1. Introduction

The Fragment Mass Analyzer (FMA) is being constructed for use in heavy-ion experiments with the ATLAS superconducting linear accelerator system at Argonne National Laboratory. It is a triple-focussing recoil mass spectrometer, designed to separate nuclear reaction recoils from the primary heavy-ion beam and disperse them in M/Q (mass/unit charge) at the focal plane.

The main ion-optical elements are two electric dipoles and a magnetic dipole, with the electric dipoles (E) symmetrically placed before and after the magnet (M). The elements are spaced such that the position energy dispersion (x/δ_E) and the angle energy dispersion (θ/δ_E) of the system both vanish (energy focus). Here δ_E stands for $\Delta E/E$, the fractional energy deviation from the central energy. The energy-dispersionless EME configuration was first used by Cormier and Stwertka [1,2] for the Recoil Mass Spectrometer at Rochester, and was also chosen by Spolaore et al. [3] for the Recoil Mass Spectrometer (RMS) at the Laboratori Nazionali di Legnaro (LNL) in Padua. Although the energy dispersion is cancelled, the M/Q dispersion is not, and the device performs as a mass spectrometer. When used in the energy-dispersionless mode, the EME combination of elements offers some distinct advantages over designs containing Wien filters [4] (superimposed EM) or a single electrostatic element [5] (ME). These advantages include wider M/Q and energy acceptances and superior rejection of the primary beam ($\sim 10^{-12}$). The energy focus condition implies isochronous orbits for particles having the same M/Q and energy but with differing emission angles at the target, an important feature when used with pulsed beam accelerators like ATLAS.

Additional magnetic elements like quadrupole singlets (Q) and sextupoles (S) are commonly used in these devices to accomplish the geometrical focussing and to provide some second-order corrections. The Rochester device has the configuration QQQEMEQQQ, while the LNL RMS has the configuration QQESMSE. Other configurations that have been proposed include QQEMMEQQ by Wilhelm [6] for the LARA spectrometer at Munich, and QQEMEQQQ by Cole et al. [7] for a spectrometer at Oak Ridge.

2. Scientific Program

The FMA will be used in a number of different experimental programs. One example is to select a particular reaction channel in studies of high-spin states in nuclei. This will allow the study of weak reaction channels in the presence of very high-yield background reactions. The FMA serves as an M/Q gate for prompt gamma-rays detected at the target using the Argonne-Notre Dame BGO-Compton-Suppressed Spectrometer array. Detectors at the focal plane will identify the mass, and in some cases, the atomic number Z of the incident recoil ions, using position, time-of-flight, and energy loss. Subsidiary detectors near the target, such as a neutron wall, can also aid in the Z identification.

Another class of experiments benefitting from the FMA is the study of short-lived radioactive nuclei far from stability. Since a typical recoil ion travels through the FMA in about 1 microsecond, very short half-lives can be observed. Techniques such as implantation into position-sensitive Si detectors and tape transport systems will be used in these experiments. Both neutron-deficient and neutron-rich species can be produced at ATLAS. A variation on these experiments is the study of nuclear moments using a beam of radioactive ions behind the FMA focal plane.

Reaction-mechanism studies are also possible using the FMA. Proposed measurements include incomplete fusion, sub-barrier fusion, and resonances in quasi-elastic scattering, using the detection of target-like residues.

3. Ion Optics

After a design study where a number of such configurations were compared, the symmetric configuration QQEMEQQ was chosen for the FMA. Figure 1 shows an outline of the device. The calculated ion optics are shown in Figure 2, and Figure 3 shows a calculated M/Q spectrum near mass 100. The matrix ion-optical code GIOS was used for these calculations. The dispersion used in Fig. 3 was 10 mm/%. This gives a spacing of 10 mm between adjacent masses at A = 100, which is easily within the capability of modern position-sensitive detectors.

There are a number of similarities and a number of differences between the ion optics of the FMA and the LNL RMS. The magnetic dipoles of both devices use a 7° pole edge rotation angle, and also curved pole edges to introduce a second-order correction. In the case of the RMS, the pole edge angle provides some vertical focussing in addition to that available from the quadrupole. In the FMA, a vertical crossover in the magnet means that all vertical focussing is done by the quadrupoles. For both devices, weaker horizontal focussing resulting from the 7° pole rotation angle serves to provide more space between the electric and magnetic dipoles than is mandated by the energy focus condition with flat pole edges. This allows room for bellows, pumping ports, and diagnostic equipment.

The extra quadrupole doublet in the FMA introduces an additional degree of freedom, allowing the M/Q dispersion to be made variable. The RMS has two sextupole magnets located in the spaces between the magnetic and electric dipoles. These are used to rotate the focal plane so that it is perpendicular to the optic axis of the device. In the FMA the depth of focus is sufficiently great that this rotation was felt to be unnecessary, and thus no sextupole lenses are used. Finally, the extra vertical control introduced by the second quadrupole doublet in the FMA provides a vertical beam spot size smaller than that of the RMS by about a factor of three. This is offset by a slightly smaller M/Q range at the focal plane, even though the quadrupole has a 15 cm bore.

There are three principal second-order aberrations in the FMA: (x/δ_E^2), $(x/\theta\delta_E)$, and (x/θ^2). The first has been set to zero by choosing the radius of curvature of the pole edges of the magnet to be 2.8 m. Figure 4 shows that this action has reduced the second aberration considerably as well, but has raised the (x/θ^2) coefficient to a value which makes it the principal limitation on the M/Q resolution. This fact can be used as an advantage by the experimenters, since the M/Q resolution can be improved quadratically with decreasing horizontal acceptance angle, while the solid angle will only decrease linearly.

Table I gives some of the properties of the FMA. The solid angle, M/Q acceptance, and energy acceptance are slightly smaller than the corresponding values for the LNL RMS, almost entirely due to the fact that the electrode gap in the FMA electric dipoles has been set to 100 mm instead of 150 mm. All peak magnetic fields have been chosen such that the upper bending limit on recoil ions is set by the voltages obtained with the electric dipoles.

4. Mechanical Design and Construction

The FMA will be mounted on a platform that will allow continuous positioning at angles between -5° and +45° to the beam direction. In addition, the entire device will be able to move in a radial direction over a total distance of approximately 0.5 meter. This will allow a variation in the distance between the target and the first quadrupole from about 10 to 60 cm, thus permitting the placement of large detector arrays around the target or larger solid angle for those experiments requiring it.

The problem of conducting high voltages into the electric dipole vacuum chambers has been solved in an unconventional fashion. Based on a similar installation for the MIT-Oak Ridge Velocity Filter, [8] the Cockroft-Walton multiplier stacks will be placed in SF_6-pressurized ceramic containers inside the vacuum chambers, making direct contact at the high-voltage end with the electrodes. By eliminating high-voltage bushings, damping resistors, and coaxial cabling from an external high-voltage supply, the amount of stored energy is greatly reduced, diminishing the potential for electrode damage during a spark. The multipliers are driven by a commercial RF high-voltage supply, and have proven to be extremely robust. In test runs, a total voltage of 480 kV (± 240 kV) over a gap of 94 mm between two aluminum test electrodes was achieved. In addition, a single electrode at 225 kV was bombarded by a 50-na 70-MeV $^{12}C^{5+}$ beam from ATLAS. No discernible voltage change at the level of a few parts in 10^5 was observed, while at the same time the supply current was observed to decrease by about 50 na, as expected.

To accommodate the expected high beam currents from the positive-ion upgrade to ATLAS, provision is being made for cooling the anode of the first electric dipole. It should be recalled that the primary beam will be dumped on this plate. Cooling will be accomplished by circulating a dielectric fluid through a suitable closed-circuit system in intimate contact with the rear surface of the electrode.

As has been mentioned previously, the energy focus condition manifests itself through the required separation distance between the electric and magnetic dipoles. All reasonable care will be taken to place these devices in the correct positions. This requires precise knowledge of the position of the effective field boundaries for each dipole. A limited adjustment capability will be provided by movable field clamps on the magnetic dipole. However, in order to most easily set up the energy focus, an additional adjustment is desirable. Using correction coils constructed of ordinary fiberglass circuit board, a variable quadrupole component will be superimposed on the dipole field of the 40° magnet. This adjustment is equivalent to a variation of the pole edge rotation angle, and also therefore of the focal length of the magnet. Tests will be done with an alpha source and heavy ion beams from the accelerator.

Finally, an FMA user group has been formed, with the intent of having some of the needed experimental facilities designed and constructed at user institutions. These include a neutron multiplicity detector for the target area, focal-plane detectors, a tape transport system, and a nuclear spectroscopy/nuclear moments facility to be located downstream from the focal-plane area.

5. Status Report (September 1988)

A new 2700 ft^2 addition to the ATLAS target room is currently under construction. The FMA will be housed in this area, along with one or two other target lines. An order for the 40° magnet, quadrupoles, electric dipoles, NMR, and magnet power supplies has been placed with Bruker Instruments of Karlsruhe, W. Germany, who is also the manufacturer of the RMS. Delivery is expected during the summer of 1989. Construction of the support structure will begin as soon as specific details on supporting the major elements are received from the manufacturer. Work will continue on testing the high-voltage power supplies, with a full-wave prototype to be constructed later this year. Upon completion of the building in the spring of

1989, the support structure will be installed. Ion-optical elements will be tested and installed in late 1989, along with the vacuum system. It is hoped that preliminary tests of the whole system can begin in early 1990, and first experiments shortly thereafter.

References

[1] T. M. Cormier and P. M. Stwertka, Nucl. Instrum. Meth. 184, 423 (1981).

[2] T. M. Cormier, M. G. Herman, B. S. Lin and P. M. Stwertka, Nucl. Instrum. Meth. 212, 185 (1983).

[3] Paola Spolaore, James Daniel Larson, Cosimo Signorini, Silvio Beghini, Zhu Xi-Kai and Si Hou-Zhi, Nucl. Instrum. Meth. A238, 381 (1985).

[4] A. N. James, T. P. Morrison, K. L. Ying, K. A. Connell, H. G. Price and J. Simpson, Nucl. Instrum. Meth. A267, 144 (1988).

[5] S. Morinobu, I. Katayama and H. Nakabushi, Proc. 4th Intern. Conf. on Nuclei Far from Stability, Helsingor, June 1981, CERN 81-09, Eds. P. G. Hansen and O. B. Nielsen, p. 717.

[6] W. Wilhelm, private communication (1987).

[7] J. D. Cole, T. M. Cormier, J. H. Hamilton and A. V. Ramayya, Proc. 5th Intern. Conf. on Nuclei Far from Stability, Rosseau Lake, September 1987, AIP Conf. Proceedings 164 (1988), Ed. I. S. Towner, p. 835.

[8] J. L. Blankenship, private communication (1986).

Table I. FMA Dimensions and Capabilities

Overall length	8.2m

Dipoles	MD	ED1, ED2
Radius of curvature	1 m	4 m
Deflection angle	40°	20°
EFB* shim angles	7°	0°
EFB radii	2.8 m	--
Gap	12 cm	10 cm
Maximum field	1.0 T	45 kV/cm
Maximum rigidity (central trajectory)	1.0 T-m $\left(\frac{48.5\ \text{MeV-AMU}}{Q^2}\right)$	18 MV = (9 MeV/Q)

Magnetic Lenses	Q1	Q2	Q_3, Q_4
Diameter (cm)	10	10	15
Effective length (cm)	30	20	30
Max. field at pole tip (T)	0.8	0.8	0.8

M/Q range	±6%
Energy range (ΔE)	±15%
Solid angle acceptance (Ω)	≈ 8 msr
M/Q resolution (at Ω = 8 msr, ΔE = ±10%)	1/340
Dispersion	variable, typically 10 mm/%
Time dispersion	<0.06%

*Effective Field Boundary.

Figure Captions

Fig. 1 Outline of the FMA. Beam is incident from the left.

Fig. 2 Calculated ion optics for the FMA.

Fig. 3 Calculated M/Q spectrum at mass 100.

Fig. 4 Principal ion-optical aberrations of the FMA. The abscissa is 1/R, where R is the radius of curvature of the entrance and exit pole edges of the 40° magnet.

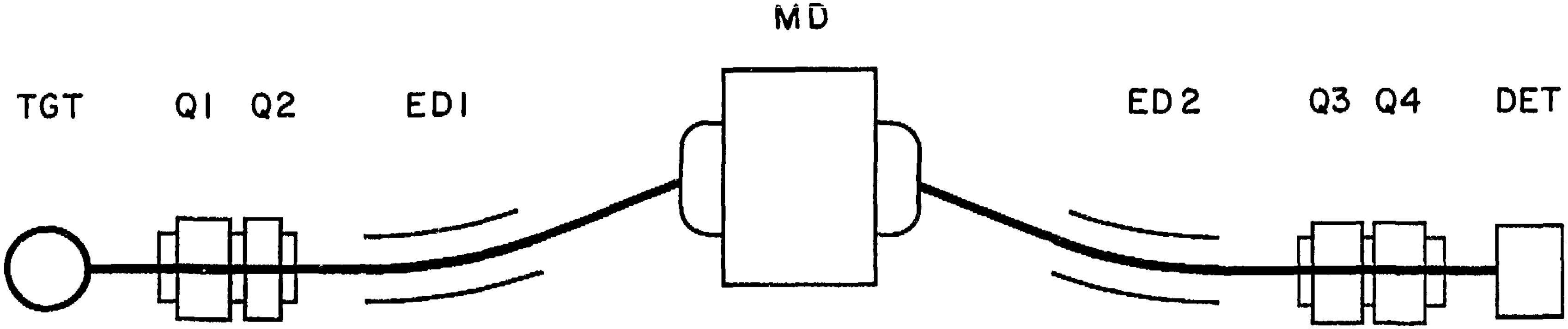
TGT
QI
Q2
EDI
MD
ED2
Q3
Q4
DET

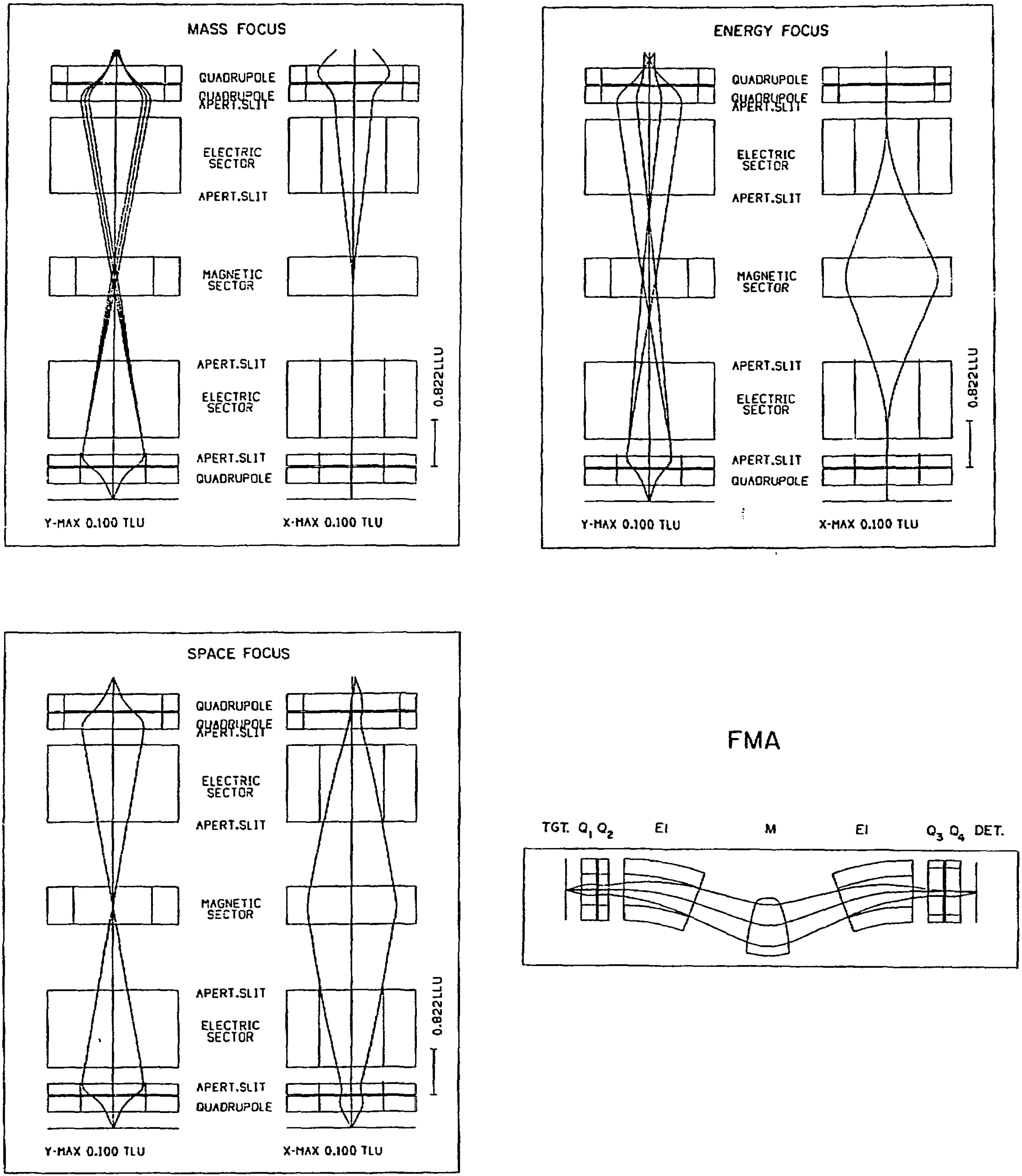
MASS FOCUS
QUADRUPOLE
QUADRUPOLE
APERT.SLIT
ELECTRIC SECTOR
APERT.SLIT
MAGNETIC SECTOR
APERT.SLIT
ELECTRIC SECTOR
APERT.SLIT
QUADRUPOLE
0.822LLU
Y-MAX 0.100 TLU
X-MAX 0.100 TLU
ENERGY FOCUS
QUADRUPOLE
QUADRUPOLE
APERT.SLIT
ELECTRIC SECTOR
APERT.SLIT
MAGNETIC SECTOR
APERT.SLIT
ELECTRIC SECTOR
APERT.SLIT
QUADRUPOLE
0.822LLU
Y-MAX 0.100 TLU
X-MAX 0.100 TLU
SPACE FOCUS
QUADRUPOLE
QUADRUPOLE
APERT.SLIT
ELECTRIC SECTOR
APERT.SLIT
MAGNETIC SECTOR
APERT.SLIT
ELECTRIC SECTOR
APERT.SLIT
QUADRUPOLE
0.822LLU
Y-MAX 0.100 TLU
X-MAX 0.100 TLU
FMA
TGT. Q_1 Q_2
El
M
El
Q_3 Q_4 DET.

Fig. 2

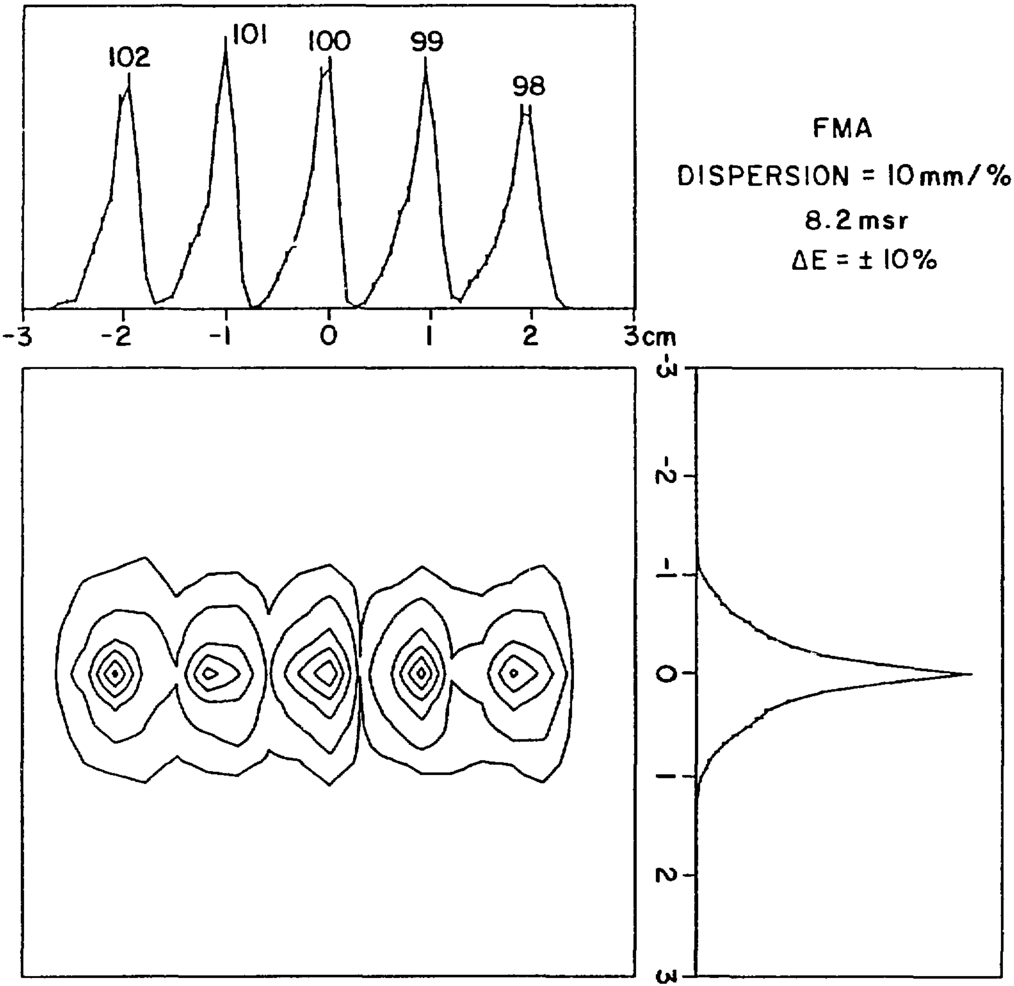

FMA
DISPERSION = 10mm/%
8.2msr
ΔE = ± 10%

CONTOURS: 2%, 10%, 30%, 50%, 70%, 90%
OF PEAK INTENSITY

Fig. 3

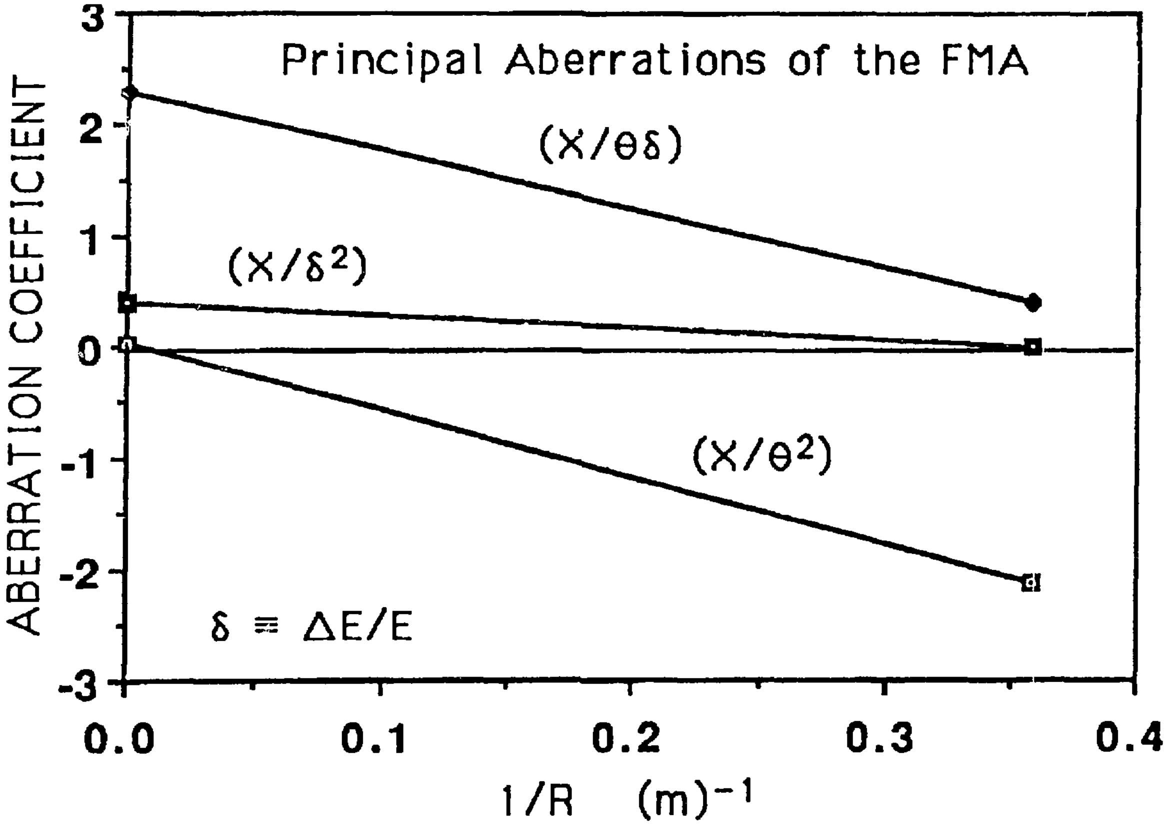

Principal Aberrations of the FMA
(X/θδ)
(X/δ²)
(X/θ²)
δ ≡ ΔE/E
ABERRATION COEFFICIENT
3
2
1
0
-1
-2
-3
0.0
0.1
0.2
0.3
0.4
1/R (m)⁻¹

Fig. 4